OPEN

see commentary on page 496

Pharmacological activation of NQO1 increases NAD^+ levels and attenuates cisplatin-mediated acute kidney injury in mice

Gi-Su Oh[1,6], Hyung-Jin Kim[1,6], Jae-Hyuck Choi[1], AiHua Shen[1], Seong-Kyu Choe[1], Anzani Karna[1], Seung Hoon Lee[2], Hyang-Jeong Jo[3], Sei-Hoon Yang[4], Tae Hwan Kwak[2], Chul-Ho Lee[5], Raekil Park[1] and Hong-Seob So[1]

[1]Center for Metabolic Function Regulation, Department of Microbiology, Wonkwang University School of Medicine, Iksan, Republic of Korea; [2]Life Science Research Center, KT&G Life Sciences, Suwon, Republic of Korea; [3]Department of Pathology, Kunsan Medical Center of Wonkwang University Hospital, Kunsan, Republic of Korea; [4]Department of Internal Medicine, Wonkwang University School of Medicine, Iksan, Republic of Korea and [5]Laboratory Animal Center, Korea Research Institute of Bioscience and Biotechnology, University of Science and Technology, Daejeon, Republic of Korea

Cisplatin is a widely used chemotherapeutic agent for the treatment of various tumors. In addition to its antitumor activity, cisplatin affects normal cells and may induce adverse effects, such as ototoxicity, nephrotoxicity, and neuropathy. Various mechanisms, such as DNA adduct formation, mitochondrial dysfunction, oxidative stress, and inflammatory responses, are critically involved in cisplatin-induced adverse effects. As NAD^+ is a cofactor for various enzymes associated with cellular homeostasis, we studied the effects of increased NAD^+ levels by means of NAD(P)H:quinone oxidoreductase 1 (NQO1) activation using a known pharmacological activator (β-lapachone) in wild-type and $NQO1^{-/-}$ mice on cisplatin-induced renal dysfunction *in vivo*. The intracellular NAD^+/NADH ratio in renal tissues was significantly increased in wild-type mice co-treated with cisplatin and β-lapachone compared with the ratio in mice treated with cisplatin alone. Inflammatory cytokines and biochemical markers for renal damage were significantly attenuated by β-lapachone co-treatment compared with those in the cisplatin alone group. Notably, the protective effects of β-lapachone in wild-type mice were completely abrogated in $NQO1^{-/-}$ mice. Moreover, β-lapachone enhanced the tumoricidal action of cisplatin in a xenograft tumor model. Thus, intracellular regulation of NAD^+ levels through NQO1 activation might be a promising therapeutic target for the protection of cisplatin-induced acute kidney injury.

Kidney International (2014) **85,** 547–560; doi:10.1038/ki.2013.330; published online 11 September 2013

KEYWORDS: cisplatin; NAD^+; nephrotoxicity; NQO1; sirtuins

Correspondence: *Hong-Seob So, Center for Metabolic Function Regulation, Department of Microbiology, Wonkwang University School of Medicine, 344-2 Shinyong-dong, Iksan, Jeonbuk 570-749, Republic of Korea. E-mail: jeanso@wku.ac.kr*

[6]These authors contributed equally to this work as first authors.

Received 4 January 2013; revised 10 June 2013; accepted 13 June 2013; published online 11 September 2013

cis-Diamminedichloroplatinum II (CDDP, cisplatin) is a widely used chemotherapeutic drug for the treatment of various solid tumors in the head and neck, bladder, lung, ovaries, testicles, and uterus.[1–6] However, the use of cisplatin is limited owing to its various adverse effects, including ototoxicity, nephrotoxicity, and peripheral neuropathy, during the course of chemotherapy. Approximately one out of three patients experience a significant reduction in renal function following cisplatin treatment.[7,8] In addition to DNA damage, a positive feedback loop between inflammatory cytokines and oxidative stress causing tubular toxicity and vascular injury has been reported as the major cause of cisplatin-induced renal dysfunctions.[9–13] Post-translational modification of nuclear factor (NF)-κB p65 and p53, including phosphorylation and acetylation, may be an important factor in cisplatin-mediated cytotoxicity, because activation of these molecules has been linked to both inflammatory responses and apoptosis.[14–16] Furthermore, oxidative stress, particularly hydroxyl radical, has a major role in cisplatin-induced p53 activation through DNA damage.[6] In particular, activation of p53 by its acetylation was also critically involved in cisplatin-induced renal injury.[17]

NADH: quinone oxidoreductase 1 (NQO1) is a cytosolic antioxidant flavoprotein that catalyzes the reduction of quinones to hydroquinones by utilizing NADH as an electron donor, which consequently increases intracellular NAD^+ levels.[18,19] In addition, there is evidence that NQO1 has a role in other biological activities, including anti-inflammatory processes, the scavenging of superoxide anion radicals, and the stabilization of p53 and other tumor-suppressor proteins.[20–26] Several activators of the NQO1 enzyme have been identified, of which β-lapachone (3,4-dihydro-2,2-dimethyl-2*H*-naphto[1,2-b]pyran-5,6-dione; βL) is the best known.[27,28] βL was first isolated from the bark of the lapacho tree and reported to inhibit tumor growth.[29] However, recent reports indicate that the enzymatic activation of NQO1 by βL

has beneficial effects on several characteristics of metabolic syndromes, for example, prevention of health decline in aged mice, amelioration of obesity or hypertension, prevention of arterial restenosis, and protection against salt-induced renal injury.[30–35] Consistent with these reports, cellular NAD^+ and NADH levels have been shown to be important mediators of energy metabolism and cellular homeostasis.[36–39] As NAD^+ acts as a cofactor for various enzymes, including sirtuins (Sirts), poly(ADP-ribose) transferases, and cyclic ADP–ribose synthases,[40–43] the regulation of NAD^+ may have therapeutic benefits through its effect on NAD^+-dependent enzymes. In particular, several Sirt proteins are NAD^+-dependent protein deacetylases that have been reported to be anti-aging molecules associated with calorie restriction.[44,45] In mammals, there are seven homologs of Sir2 (Sirt1–7) that show differential subcellular localizations.[38,45] Among these, nuclear-localized Sirt1 is activated under energy stress conditions, such as fasting, exercise, or low glucose availability.[46] Sirt1 has a key role in metabolism, development, stress response, neurogenesis, hormone responses, and apoptosis[47,48] by deacetylation of substrates, such as NF-κB p65, FOXO, p53, and histones.[49–52] In addition, recent studies suggest that Sirt1 regulates inflammatory responses through NF-κB p65 deacetylation. In the absence of Sirt1 *in vivo* (knockout mice), there is deregulated inflammatory pathway activation in conjunction with increased inflammatory gene expression.[53]

Mitochondria-localized Sirt3 regulates adaptive thermogenesis, mitochondrial function, energy homeostasis, and cellular survival upon genotoxic stress.[54–56] Sirt3 exerts antioxidative effects through the deacetylation and activation of mitochondrial isocitrate dehydrogenase 2 (IDH2) and the enhancement of the glutathione antioxidant defense system. Furthermore, Sirt3 antagonizes p53 function through direct interaction and subsequent deacetylation of p53 in the mitochondria.[57]

Although a link between NAD^+-dependent molecular events and cellular metabolism is evident, it remains unclear whether modulation of NAD^+ levels has an impact on cisplatin-induced renal injury. In this study, we investigated the protective effects of βL on cisplatin-induced acute kidney injury in wild-type (WT) compared with NQO1 knockout ($NQO1^{-/-}$) mice. We found that βL protects against cisplatin-induced renal dysfunction and that this effect is mediated by Sirt1 and Sirt3 through NQO1 activation.

RESULTS

βL activates NQO1 enzyme activity and increases the intracellular ratio of NAD^+ to NADH in mice

Kidney homogenates from WT mice were isolated and treated with βL to measure NQO1 activity. As shown in Supplementary Figure S1A online, NQO1 activity was significantly increased by βL treatment (26.3 ± 2.1 vs. 11.3 ± 1.2 nmol/min/mg protein (control)), whereas it was attenuated to the control level by the addition of the NQO1 inhibitor dicumarol (14.5 ± 1.5 nmol/min/mg protein). By contrast, dicumarol itself completely abrogated NQO1 activity (1.5 ± 1.0 nmol/min/mg protein). Next, we asked whether NQO1 activation correlates with intracellular NAD^+ and NADH levels in kidney tissues. WT mice were orally administered βL or vehicle for 4 days, and NAD^+/NADH ratios were determined from isolated kidney tissues. We found a significant increase in the NAD^+/NADH ratio in βL-treated mice compared with the ratio in control mice (2.13 ± 0.42 vs.1.22 ± 0.3) (Supplementary Figure S1B online).

βL inhibits cisplatin-induced acute kidney injury in mice

C57BL/6 mice were treated with βL, cisplatin, or βL + cisplatin, as indicated in Supplementary Figure S2 online, and the levels of serum creatinine and blood urea nitrogen (BUN) (biochemical markers for kidney dysfunction) were measured at day 4. As shown in Figure 1a and b, cisplatin increased the levels of serum creatinine and BUN (1.67 ± 0.12 and 126 ± 7.5 mg/dl, respectively), compared with control (0.31 ± 0.11 and 36.0 ± 7.4 mg/dl, respectively). However, βL + cisplatin significantly reduced the levels of both serum creatinine (1.01 ± 0.15 mg/dl) and BUN (79.8 ± 4.1 mg/dl), as

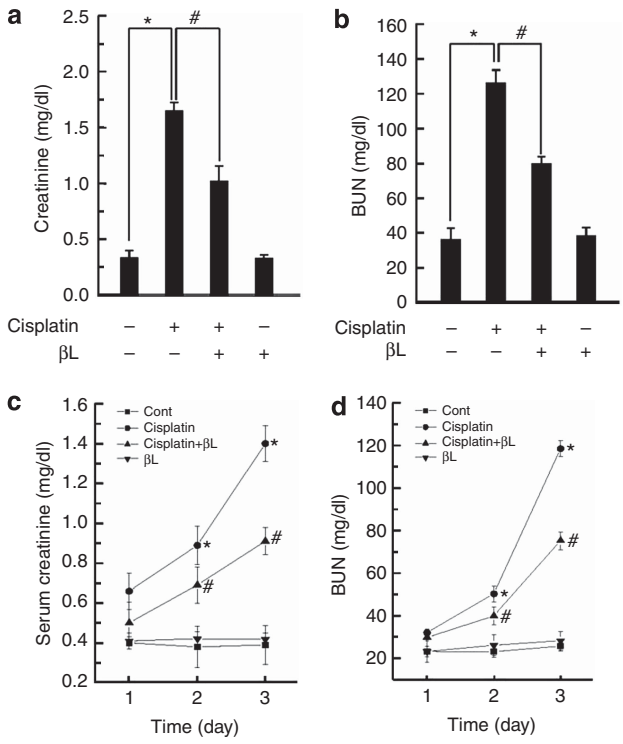

Figure 1 | Effect of β-lapachone (βL) on serum creatinine and blood urea nitrogen (BUN) in cisplatin-induced acute kidney injury. βL (40 mg/kg body weight) was administered orally once a day for 4 consecutive days. Cisplatin (20 mg/kg body weight) was injected once at 12 h after the first βL administration. The mice were killed at 72 h after the single cisplatin injection, and levels of (**a**) serum creatinine and (**b**) BUN were analyzed using an assay kit according to the manufacturer's instructions (BioVision). To observe the effect of βL on the cisplatin-induced toxicity with the experimental time course, the mice were killed daily after cisplatin injection, and serum was analyzed for (**c**) creatinine and (**d**) BUN. $^{*,\#}P < 0.05$ by one-way analysis of variance compared with the control (*) and cisplatin + βL group (#) ($n = 5$).

compared with cisplatin alone. Levels in βL-treated and control mice were similar. In addition, to determine the time-dependent effect of βL on cisplatin-induced acute kidney injury, we examined the kidney function for 3 consecutive days after cisplatin or cisplatin + βL administration. As shown in Figure 1c and d, cisplatin-induced serum creatinine and BUN were suppressed by βL treatment in a time-dependent manner. These results suggest that βL may protect against cisplatin-induced kidney dysfunction.

βL ameliorates cisplatin-induced renal tubular damage in mice

The pathophysiology of cisplatin-induced renal injury can be classified into four types: (i) tubular toxicity, (ii) vascular damage, (iii) glomerular injury, and (iv) interstitial injury. The multistep, complex processes that result in renal damage are caused by the concentration of potential toxic elements in the tubular fluid, which then diffuse into the highly permeable tubular cells. Cisplatin, which has a low molecular weight and is uncharged, is freely filtered at the glomeruli and subsequently taken up by renal tubular cells, ultimately reaching its highest concentrations in the proximal tubular cells of the inner cortices and outer medullae.[58] Thus, these areas are the major sites for cisplatin-induced renal damage, which, in turn, causes injury to other tubular areas, including the distal tubule and collecting tubule.[4,59,60]

To examine the tubular damage by cisplatin and the potential protective effect of βL, kidney specimens from experimental groups were stained with hematoxylin and eosin (H&E). As shown in Figure 2a, mice treated with cisplatin showed various tubular injuries, such as tubular dilation, vacuole formation, and necrosis, whereas mice treated with βL + cisplatin showed significantly reduced tubular injuries. Renal histology in βL alone was similar to that in control. Consistent with H&E staining, cisplatin-treated mice had deleterious structural changes, including loss of the brush border membrane, deposition of periodic acid–Schiff (PAS)-positive materials, and cast formation, whereas coadministration of βL abrogated these deleterious effects (Figure 2b). For quantitative comparison of tissue injury among the samples, tubular injuries were scored based on the percentage of cortical tubular necrosis described in the Methods section. As shown in Figure 2c, cisplatin significantly increased tubular injury (3.05 ± 0.605) compared with control, whereas βL significantly attenuated the cisplatin-induced tubular injury (1.1 ± 0.31). Levels in βL-treated and control mice were similar. These results suggest that βL protects against cisplatin-induced tubular injury.

βL inhibits potential mediators or processes for cisplatin-induced renal damage in mice

Because inflammatory cytokines such as tumor necrosis factor (TNF)-α, interleukin (IL)-1β, and IL-6 may relay cisplatin-induced toxicity, we examined whether the upregulation of these mediators by cisplatin is affected by βL coadministration. First, we assessed TNF-α in serum and urine as a representative mediator of the pathogenesis of cisplatin-induced acute kidney injury (Figure 3a and b). Cisplatin administration produced a robust increase in serum and urine TNF-α levels (310 ± 40 and 139 ± 2.0 pg/ml, respectively), whereas βL coadministration significantly attenuated serum and urine TNF-α levels (165 ± 22 and 73 ± 4.5 pg/ml, respectively). Serum and urine TNF-α levels in control mice (32 ± 24 and 13 ± 5 pg/ml, respectively) and βL-treated mice (77 ± 2.5 and 66 ± 2.6 pg/ml, respectively) were low. We also examined TNF-α level in kidney tissue by immunohistochemistry (IHC) and quantitative enzyme-linked immunosorbent assay (ELISA). TNF-α in cisplatin-treated kidney tissue was strongly attenuated by βL coadministration, as shown by IHC (Figure 3c). This βL-mediated attenuation of TNF-α expression was further confirmed by ELISA (Figure 3d). We also examined other proinflammatory cytokines, IL-1β and IL-6, in kidney tissue. As shown in Supplementary Figure S3 online, IL-1β and IL-6 levels were also increased by cisplatin treatment, whereas βL coadministration attenuated cisplatin-induced elevation of those cytokines.

Oxidative stress by reactive oxygen species (ROS) has also been implicated in the pathogenesis of cisplatin-induced renal injury, and membrane NAD(P)H oxidases (NOXs) are one of the major sources for ROS generation. Therefore, we analyzed the renal tissue expression of NOX1 and NOX4 in response to cisplatin, βL, or cisplatin + βL by IHC and western blotting from kidney sections and tissue lysates, respectively. IHC from kidney sections showed that cisplatin treatment increases the expression of NOX1 and NOX4, especially in damaged areas, whereas βL coadministration almost completely attenuated the expression of these proteins (Figure 3e and f). βL alone was similar to control. Similarly, western blot analysis showed that βL coadministration potently attenuated cisplatin-induced NOX1 and NOX4 expression levels (Figure 3g and h). Consistent with NOX expression levels, cisplatin-induced NOX enzyme activity was abrogated by βL coadministration, as shown in Figure 3i.

As the infiltration of immune cells to the site of injury is indirectly assessed by the expression level of chemokines, we evaluated monocyte chemotactic protein-1 (MCP-1), one of the well-known proinflammatory chemokines for neutrophil infiltration, in a kidney section. As shown in Figure 3j and k, βL coadministration potently inhibited MCP-1 expression induced by cisplatin. We also quantified the number of neutrophils infiltrated to the injured kidney. The number of infiltrated neutrophils was markedly increased by cisplatin administration, whereas it was completely blocked by βL coadministration (Figure 3l).

NF-κB activation acts as one of the major signals for inflammatory responses and ROS formation. Therefore, we examined NF-κB p65 expression by IHC and western blotting. Increased expression of NF-κB p65 was clearly observed by IHC in the renal tubular area of cisplatin-treated mice, whereas βL co-treatment attenuated this expression (Figure 3m). For the quantitative analysis of NF-κB

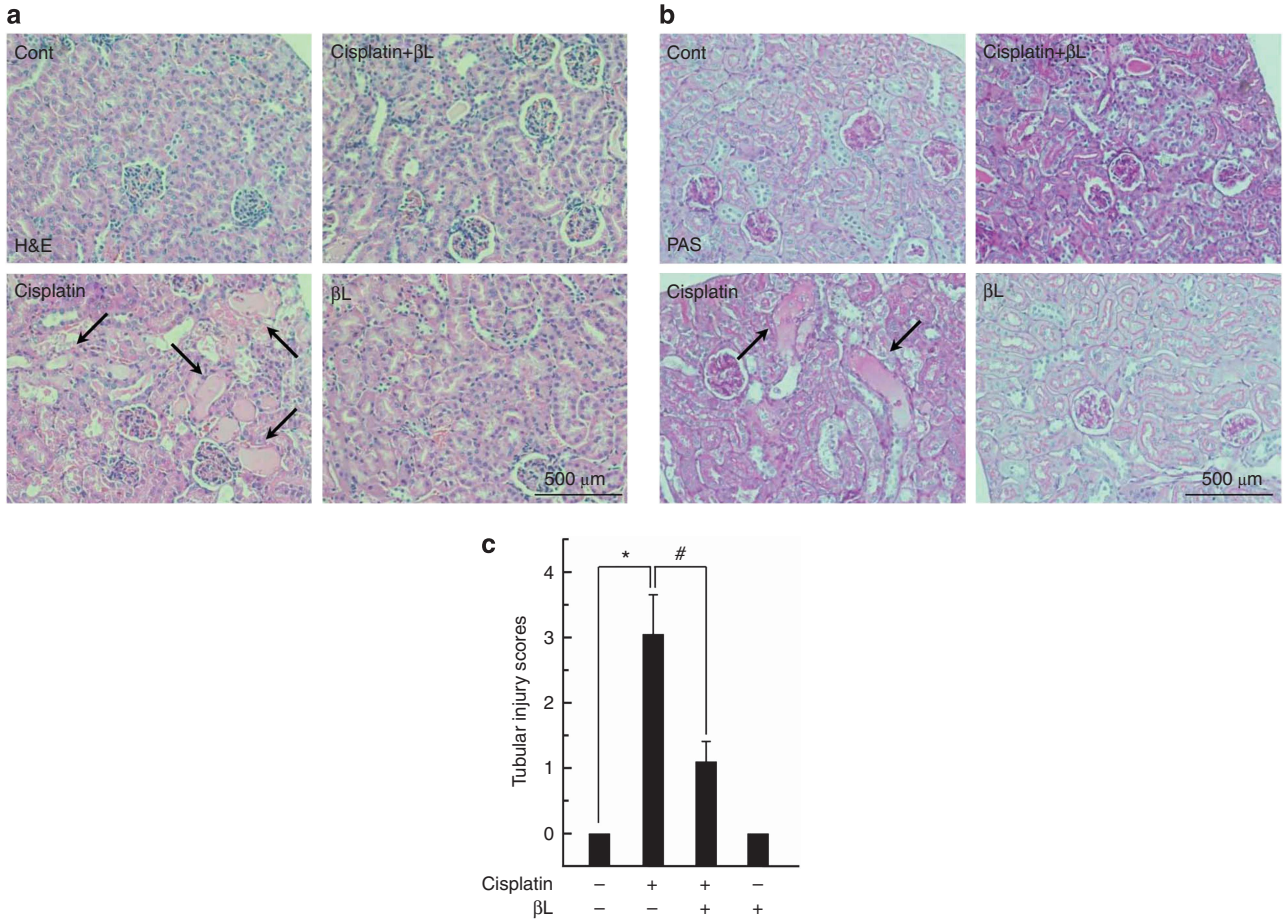

Figure 2 | Effect of βL on renal histology in cisplatin-induced acute kidney injury. Kidney specimens were stained with hematoxylin and eosin (H&E) and periodic acid–Schiff (PAS) and the tubular injury was quantified. (**a**) H&E staining. Cont, PBS (phosphate-buffered saline)-treated control group; cisplatin, 20 mg/kg cisplatin only group; cisplatin + βL, cisplatin and 40 mg/kg βL combined group; βL, βL only group. (**b**) PAS staining. Damaged areas on tissue sections are marked with black arrows. (**c**) Tubular injury was scored using the quantitative evaluation method as described in the Methods. $^{*,\#}P < 0.001$ by one-way analysis of variance compared with the control (*) and cisplatin + βL group (#) ($n = 10$).

activation, we examined p65 nuclear translocation by western blotting using the nuclear fraction of kidney tissues. As shown in Figure 3n and o, cisplatin-induced p65 nuclear translocation was significantly reduced by βL coadministration. Taken together, these results strongly suggest that βL prevents cisplatin-induced acute kidney injury by suppressing critical mediators for inflammation and ROS.

NQO1 mediates βL-induced renal protection in cisplatin-treated mice

We investigated whether βL-induced protective effects are mediated through NQO1 activation. We performed a series of experiments using NQO1$^{-/-}$ mice, similar to those shown in Figures 1–3 using WT mice. We analyzed the biochemical markers and histology of renal injury in cisplatin-treated NQO1$^{-/-}$ mice (Figure 4a–e). The levels of serum creatinine and BUN (1.65 ± 0.26 and 144 ± 10.0 mg/dl, respectively) in cisplatin-treated NQO1$^{-/-}$ mice were similar to or a little higher than those observed in cisplatin-treated WT mice. As expected, βL coadministration did not reduce the levels of these markers (creatinine: 1.25 ± 0.32; BUN: 124.5 ± 13.2 mg/dl) in NQO1$^{-/-}$ mice. In the histological staining, cisplatin treatment of NQO1$^{-/-}$ mice caused typical renal damage (i.e., tubular necrosis, brush-border loss, dilation of the tubular area, and cast formation). However, unlike the WT results, βL coadministration did not protect against cisplatin-induced tubular damage in NQO1$^{-/-}$ mice (Figure 4c–e). These results suggest that the βL-induced protective effects are mediated through NQO1 activation. We also investigated TNF-α production in serum and tissue of βL and cisplatin co-treated NQO1$^{-/-}$ mice. As predicted, serum TNF-α levels were similarly increased in both cisplatin- and cisplatin + βL-treated NQO1$^{-/-}$ mice (222 ± 40 vs. 202 ± 70 pg/ml) (Figure 5a). Similarly, TNF-α expression in renal tissue was also strongly induced in both cisplatin- and cisplatin + βL-treated NQO1$^{-/-}$ mice (Figure 5b and c). Levels of other proinflammatory cytokines, IL-1β and IL-6, were not also decreased by βL coadministration in NQO1$^{-/-}$ mice (Supplementary Figure S4 online). In addition, MCP-1 expression remained elevated in NQO1$^{-/-}$ mice regardless

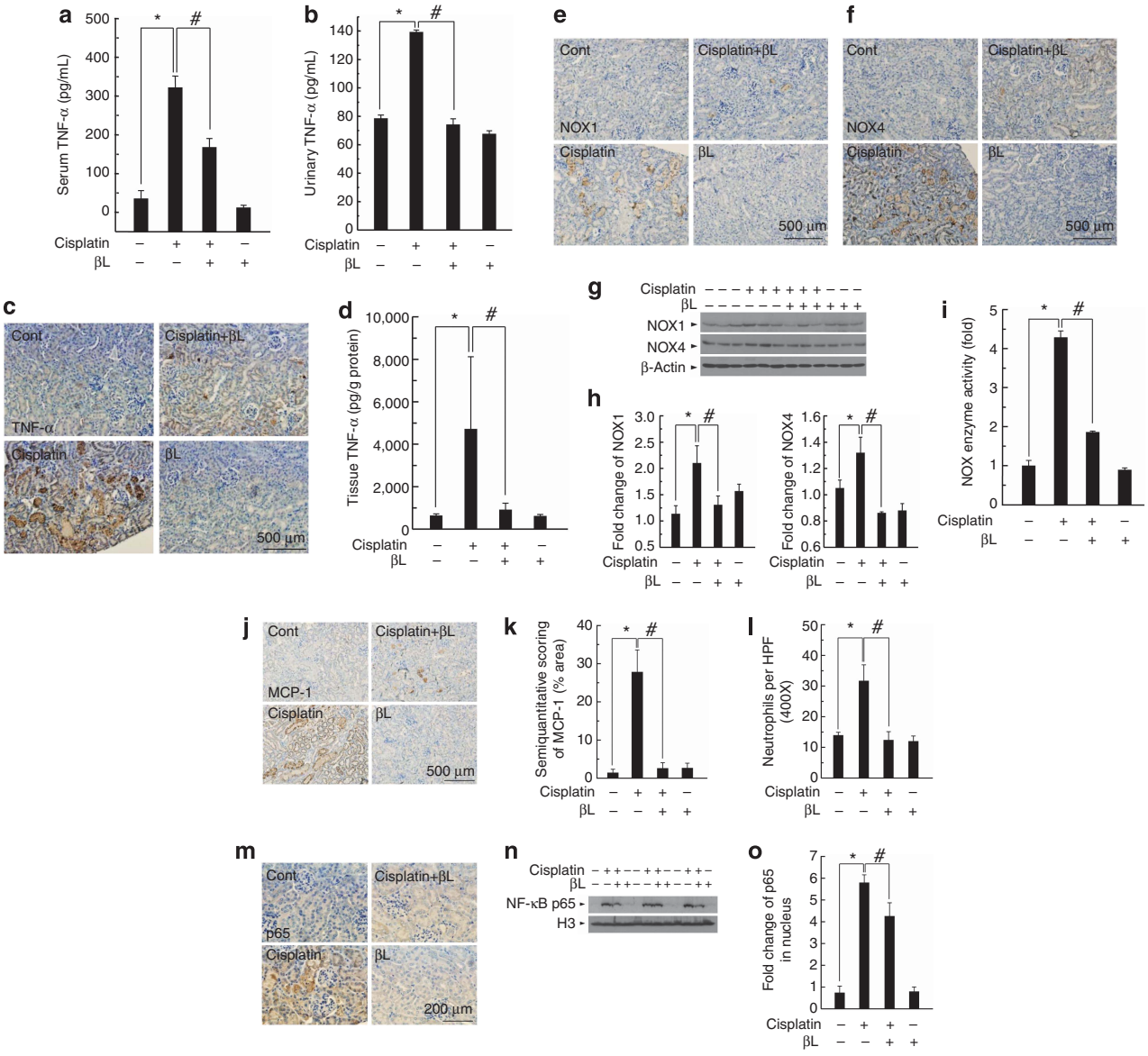

Figure 3 | Effect of βL on cisplatin-induced renal damage mediators. Tumor necrosis factor (TNF)-α was analyzed in (**a**) serum and (**b**) urine. $^{*,\#}P<0.05$ by one-way analysis of variance (ANOVA) compared with the control (*) and cisplatin + βL group (#) ($n=5$). (**c**) Kidney specimens were stained with TNF-α antibody for immunohistochemistry. Cont, PBS (phosphate-buffered saline)-treated group; cisplatin, 20 mg/kg cisplatin only treated group; cisplatin + βL, cisplatin and 40 mg/kg βL combined group; βL, βL only group. (**d**) TNF-α levels in kidney tissues were analyzed by enzyme-linked immunosorbent assay. $^{*,\#}P<0.005$ by one-way ANOVA compared with the control (*) and cisplatin + βL group (#) ($n=5$). Kidney sections were IHC-stained with (**e**) NAD(P)H oxidase 1 (NOX1), (**f**) NOX4, (**j**) monocyte chemotactic protein-1 (MCP-1), and (**m**) nuclear factor (NF)-κB p65 antibodies. For the quantitative analysis of protein expression level, kidney lysates were analyzed by western blotting for NOX1, and (**g**) NOX4 and (**h**) signal intensities were quantified. $^{*,\#}P<0.05$ by one-way ANOVA compared with the control (*) and cisplatin + βL group (#) ($n=3$). (**i**) Total NOX enzyme activity was analyzed from kidney tissue. $^{*,\#}P<0.05$ by one-way ANOVA compared with the control (*) and cisplatin + βL group (#) ($n=6$). (**k**) The level of MCP-1 expression shown in panel (**j**) was quantitatively evaluated by using the method as described in the Methods. $^{*,\#}P<0.001$ by one-way ANOVA compared with the control (*) and cisplatin + βL group (#) ($n=10$). (**l**) Infiltrated neutrophils were quantified from the periodic acid–Schiff (PAS)-stained specimens shown in panel (**b**). $^{*,\#}P<0.001$ by one-way ANOVA compared with the control (*) and cisplatin + βL group (#) ($n=10$). (**n**) NF-κB p65 nuclear translocation was examined by western blotting using the nuclear fraction of kidney tissues and (**o**) quantified. Histone H3 (H3) was used as a loading control. $^{*,\#}P<0.01$ by one-way ANOVA compared with the control (*) and cisplatin + βL group (#) ($n=3$). IHC, immunohistochemistry.

of βL coadministration (Figure 5d–e). Similarly, NOX1 and NOX4 expression levels were not abrogated by βL coadministration in NQO1$^{-/-}$ mice (Figure 5f–i). These results strongly indicate that βL acts through NQO1 to block cisplatin-induced acute kidney injury.

βL regulates the ratio of NAD$^+$ to NADH via NQO1 in renal tissue

Next, we examined the effect of βL on the cellular NAD$^+$/NADH ratio in the kidneys of cisplatin-treated WT or NQO1$^{-/-}$ mice. As shown in Figure 6a, the cellular

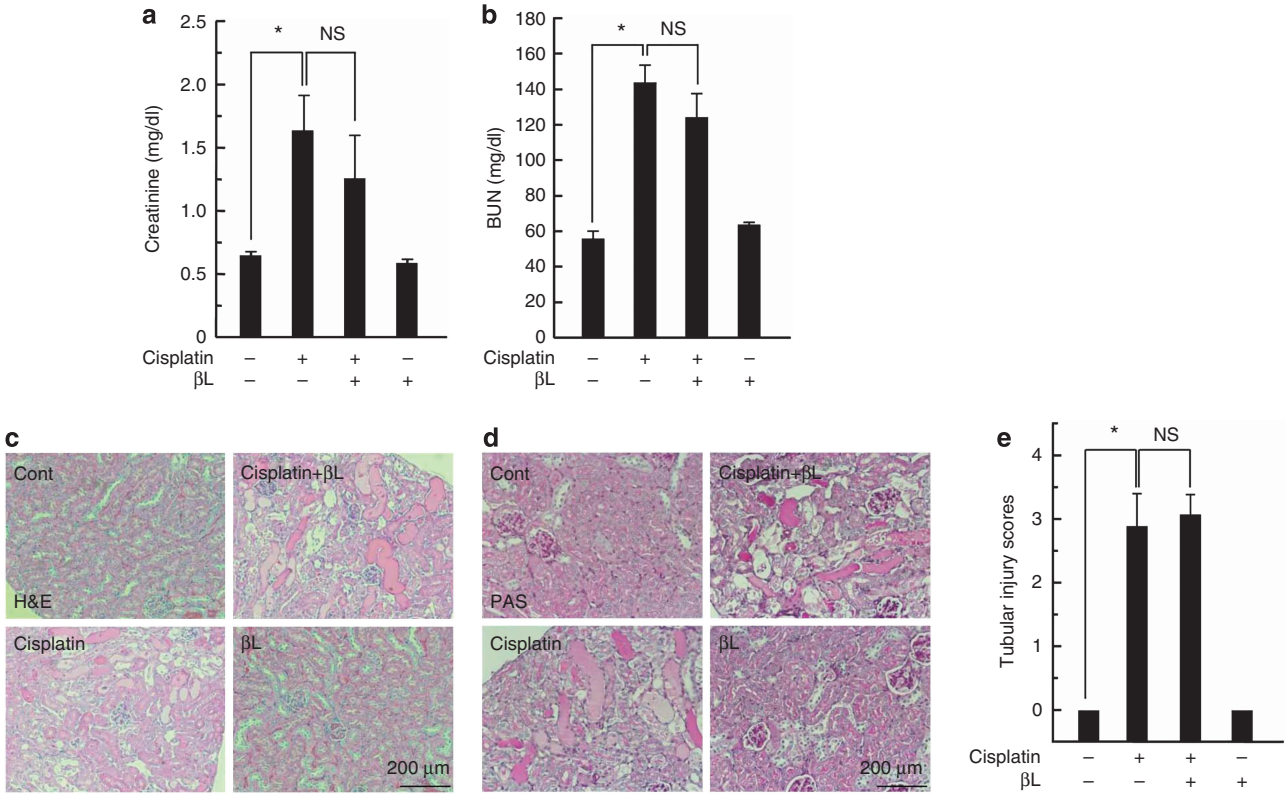

Figure 4 | Effect of βL on cisplatin-induced renal injury in NQO1$^{-/-}$ mice. βL (40 mg/kg body weight) was administered orally once a day for 4 days. Cisplatin (20 mg/kg body weight) was injected once, on the second day of βL administration. The mice were killed at 72 h after the single cisplatin injection. (**a**) Serum creatinine and (**b**) blood urea nitrogen (BUN) were measured. *$P<0.05$ by one-way analysis of variance (ANOVA) compared with the control group. Kidney sections were stained with (**c**) hematoxylin and eosin (H&E) and (**d**) periodic acid–Schiff (PAS). Cont, PBS (phosphate-buffered saline)-treated group; cisplatin, 20 mg/kg cisplatin only group; cisplatin + βL, cisplatin and 40 mg/kg βL combined group; βL, βL only group. (**e**) Tubular injury was scored using the quantitative evaluation method as described in the Methods. *$P<0.05$ by one-way ANOVA compared with the control group ($n=5$). NS, not significant.

NAD^+/NADH ratio in WT mice was lowered after cisplatin treatment compared with control (0.72 ± 0.09 vs. 1.21 ± 0.3 (control)). βL coadministration restored the cellular NAD^+/NADH ratio to control levels (1.16 ± 0.15). Interestingly, βL alone elevated the cellular NAD^+/NADH ratios in the kidney (2.12 ± 0.4) compared with control. In NQO1$^{-/-}$ mice, however, the cellular NAD^+/NADH ratio in the kidney was not affected by either cisplatin or βL alone, although the cellular NAD^+/NADH ratios in the control and βL alone groups were markedly reduced (0.59 ± 0.19 vs. 0.58 ± 0.11) compared with levels in WT mice under similar conditions (Figure 6b).

βL induces the deacetylation of NF-κB p65 and p53

It has been reported that acetylation of NF-κB p65 and p53 has significant roles in transcriptional activation of inflammation-related genes and pathological conditions associated with apoptosis. Sirt1 and Sirt3, localized in the nucleus and mitochondria, respectively, deacetylate NF-κB p65 and p53.[14–16] Therefore, we investigated the NF-κB p65 and p53 acetylation levels following cisplatin or βL coadministration as a way to indirectly estimate Sirt1 and Sirt3 activity in cisplatin-treated WT or NQO1$^{-/-}$ mice. As shown in Figure 7a and b, cisplatin-treated WT mice displayed markedly increased NF-κB p65 and p53 acetylation levels compared with control. βL coadministration significantly reduced the expression of the acetylated forms compared with cisplatin treatment alone. βL alone did not have any effect. We further confirmed by western blot analysis that the level of acetylated NF-κB p65 and p53 was strongly increased in cisplatin-treated WT mice, whereas it was significantly attenuated in cisplatin + βL co-treated WT mice (Figure 7c–d). In contrast, the attenuation of cisplatin-induced NF-κB p65 and p53 acetylation by βL treatment was not observed in NQO1$^{-/-}$ mice (Figure 7e–h). These results suggest that NQO1 is indispensible for deacetylation of NF-κB p65 and p53.

βL increases the enzymatic activities of Sirt1 and Sirt3 through NQO1 activation

Next, we examined whether βL regulates the expression and activity of Sirt1 and Sirt3. As shown in Supplementary Figure S5A–E online, IHC and western blot analyses showed that Sirt1 and Sirt3 protein expression increased in cisplatin-treated kidney tissues from WT mice, whereas it was clearly blocked by βL treatment. However, the increased expression

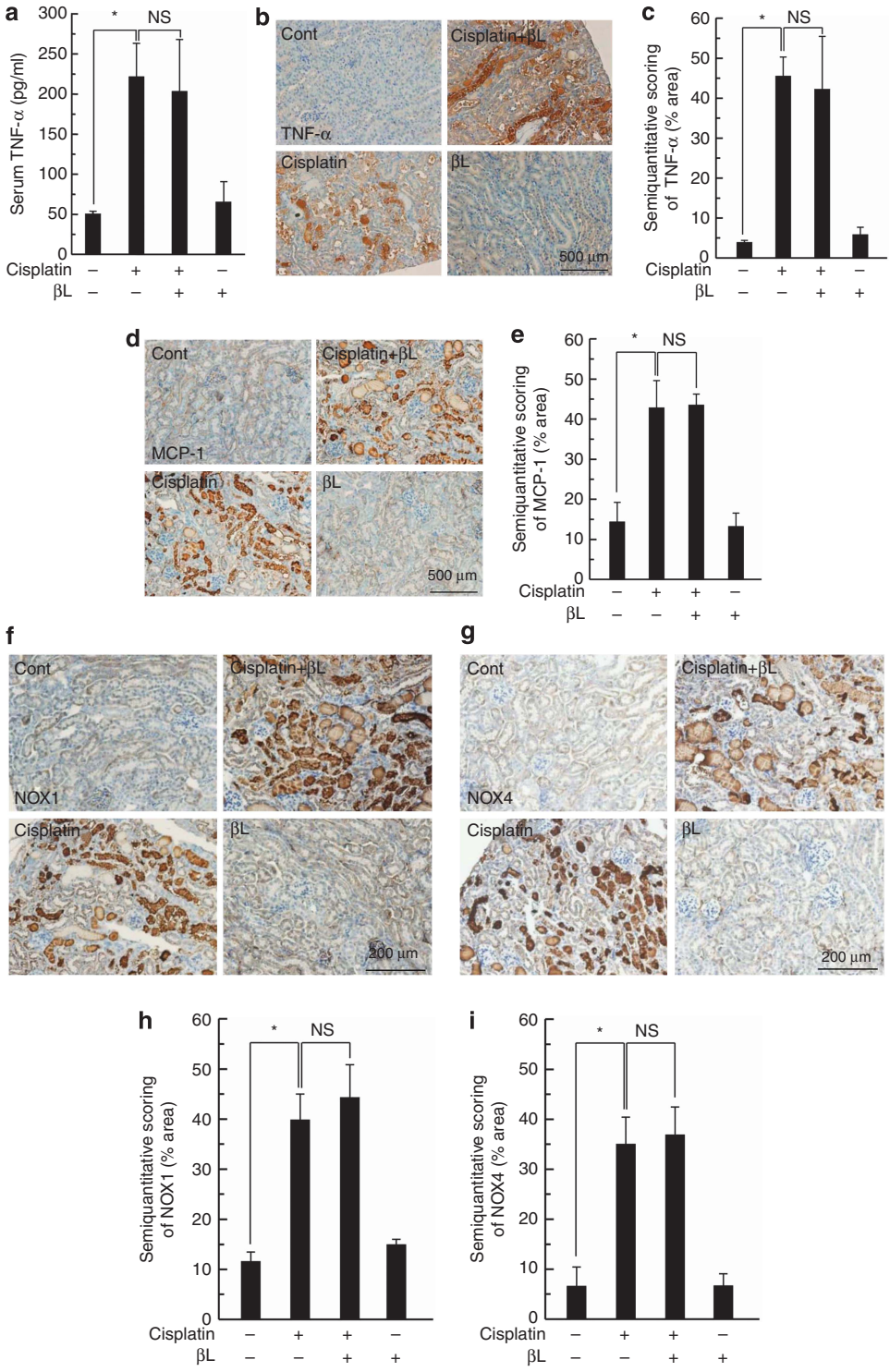

Figure 5 | Effect of βL on cisplatin-induced renal damage mediators in NQO1$^{-/-}$ mice. (**a**) Serum level of tumor necrosis factor (TNF)-α was analyzed using the enzyme-linked immunosorbent assay kit. *$P<0.05$ by one-way analysis of variance (ANOVA) compared with the control or cisplatin only group ($n=5$). Kidney sections were stained with (**b**) TNF-α, (**d**) monocyte chemotactic protein-1 (MCP-1), (**f**) NAD(P)H oxidase 1 (NOX1), and (**g**) NOX4 antibodies for immunohistochemistry (IHC). Cont, PBS (phosphate-buffered saline)-treated group; cisplatin, 20 mg/kg cisplatin only group; cisplatin + βL, cisplatin and 40 mg/kg βL combined group; βL, βL only group. IHC-processed kidney specimens were quantified for the expression levels of (**c**) TNF-α, (**e**) MCP-1, (**g**) NOX1, and (**i**) NOX4 using the ImageJ program. *$P<0.05$ by one-way ANOVA compared with the control group ($n=10$). NS, not significant.

of Sirt1 and Sirt3 induced by cisplatin was not blocked by βL in NQO1$^{-/-}$ mice (Supplementary Figure S5F–I online). Interestingly, despite a strong increase in Sirt expression in cisplatin-treated WT mice, enzymatic activities of these proteins were significantly low compared with those in control (Figure 8).

DISCUSSION

Many chemotherapeutic agents, such as cisplatin, have renotoxic side effects. Cisplatin is widely used for the treatment of various types of cancer,[6] but its use can be limited by acquired resistance and severe adverse effects in normal tissues.[2,5] The former contributes to reduced uptake, increased efflux, or neutralization of cisplatin and to defective apoptotic signaling in response to cisplatin-induced DNA damage.[5,11–13] The latter includes ototoxicity, neurotoxicity, nausea, vomiting, and nephrotoxicity. The cytotoxic mechanisms of cisplatin include oxidative stress by ROS, mitochondrial dysfunction, and the formation of DNA adducts. In addition, positive feedback loops between the secretion of TNF-α from renal tubular cells, the activation of NF-κB, and proinflammatory cytokines may also cause renal damage after cisplatin treatment.[61] Inflammatory cytokines participate in innate and adaptive immunity in the host defense system. They induce cell death through a receptor-related extrinsic mechanism. This process, in turn, elevates the production of ROS and other chemokines, which may recruit immune cells to the sites of inflammation.[62,63]

In this study, we demonstrated that βL treatment attenuates cisplatin-induced renal dysfunction by assessing the levels of serum creatinine and BUN and histology (Figures 1 and 2). In addition, βL coadministration reduces the expression of renal damage mediators, including inflammatory cytokines, the chemoattractant protein MCP-1, neutrophil infiltration, the ROS-generating proteins NOX1 and NOX4, and NOX enzymatic activity (Figure 3 and Supplementary Figure S3 online). We also demonstrated that βL downregulates the expression of NF-κB p65 and activation of NF-κB by blocking its nuclear translocation in kidney tissues (Figure 3). In addition, βL increases cellular NAD^+ levels in a NQO1-dependent manner (Supplementary Figures S1 and S6 online). These results suggest that βL may prevent cisplatin-induced acute kidney injury through NQO1 enzymatic activation and the subsequent NAD^+/NADH ratio increase. Therefore, we examined the protective role of βL coadministration in cisplatin-treated NQO1$^{-/-}$ mice. In the absence of NQO1, βL coadministration does not prevent against cisplatin-induced renal damage (Figures 4 and 5, and Supplementary Figure S4 online). Taken together, these results strongly suggest that βL protects the kidney from cisplatin-induced damage via NQO1.

NQOs are a group of flavoproteins that include NQO1 and NQO2 in mammals. Both NQO1 and NQO2 readily catalyze two electron reductions of various quinone compounds and their derivatives, resulting in the detoxification of these electrophilic compounds and the prevention of redox cycling. In addition, NQO1 possesses many other biological activities, such as scavenging of superoxide anion radicals and stabilization of the tumor-suppressor p53, which may serve as the basis for its potential involvement in protecting against disease processes.[64] However, despite these various roles of NQO1, mice lacking NQO1 gene expression showed no detectable phenotype and were indistinguishable from WT mice, although NQO1 null mice exhibited increased toxicity when administered menadione compared with WT mice.[65] It is plausible that in NQO1 null mice NQO2 may compensate for the loss of NQO1[65] and thus may not worsen renal dysfunction compared with WT even in cisplatin-induced acute kidney injury. In our study, we also found that there is no obvious difference in the extent of cisplatin-induced acute kidney injury between WT and NQO1$^{-/-}$ mice. We just used these NQO1 null mice to investigate whether the enzymatic activation of NQO1 is indispensable for the effect

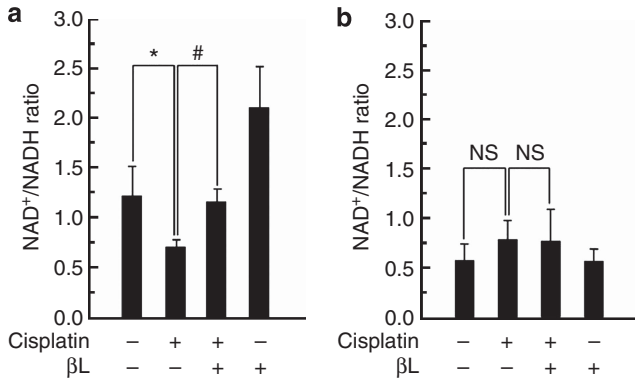

Figure 6 | Effect of βL on intracellular NAD^+/NADH ratio. Effect of βL on intracellular NAD^+/NADH ratio in cisplatin-treated (**a**) wild-type and (**b**) NQO1$^{-/-}$ mice. NAD^+ and NADH were extracted from kidney tissues as follows: control (Cont), cisplatin, cisplatin + βL, and βL only. NAD^+ and NADH concentrations were measured by using an assay kit according to the manufacturer's instructions. $^{*,\#}P<0.05$ by one-way analysis of variance compared with the control (*) and cisplatin + βL only group (#) ($n=5$). NS, not significant.

Figure 7 | Effect of βL on cisplatin-mediated acetylation of nuclear factor (NF)-κB p65 and p53 in renal tissue from wild-type (WT) and NQO1$^{-/-}$ mice. Kidneys from mice treated with phosphate-buffered saline, cisplatin, βL + isplatin, and βL alone were removed and embedded in paraffin, and 5-μm sections were prepared. Immunohistochemistry (IHC) was performed by using antibodies against the (**a**, **c**, **e**, **g**) acetylated forms of p65 and (**b**, **d**, **f**, **h**) p53 from WT (**a**, **b**) or NQO1$^{-/-}$ (**e**, **f**) mice sections. Western blot was performed, and signal intensity was quantified for p65 (**c**) and p53 (**d**). $^{*,\#}P<0.05$ by one-way analysis of variance (ANOVA) compared with the control (*) and cisplatin + βL only group (#) ($n=3$). IHC-processed kidney specimens of NQO1$^{-/-}$ mice were quantified for acetyl p65 (**g**) and p53 (**h**) using the ImageJ program. $^*P<0.05$ by one-way ANOVA compared with the control group ($n=5$). NS, not significant.

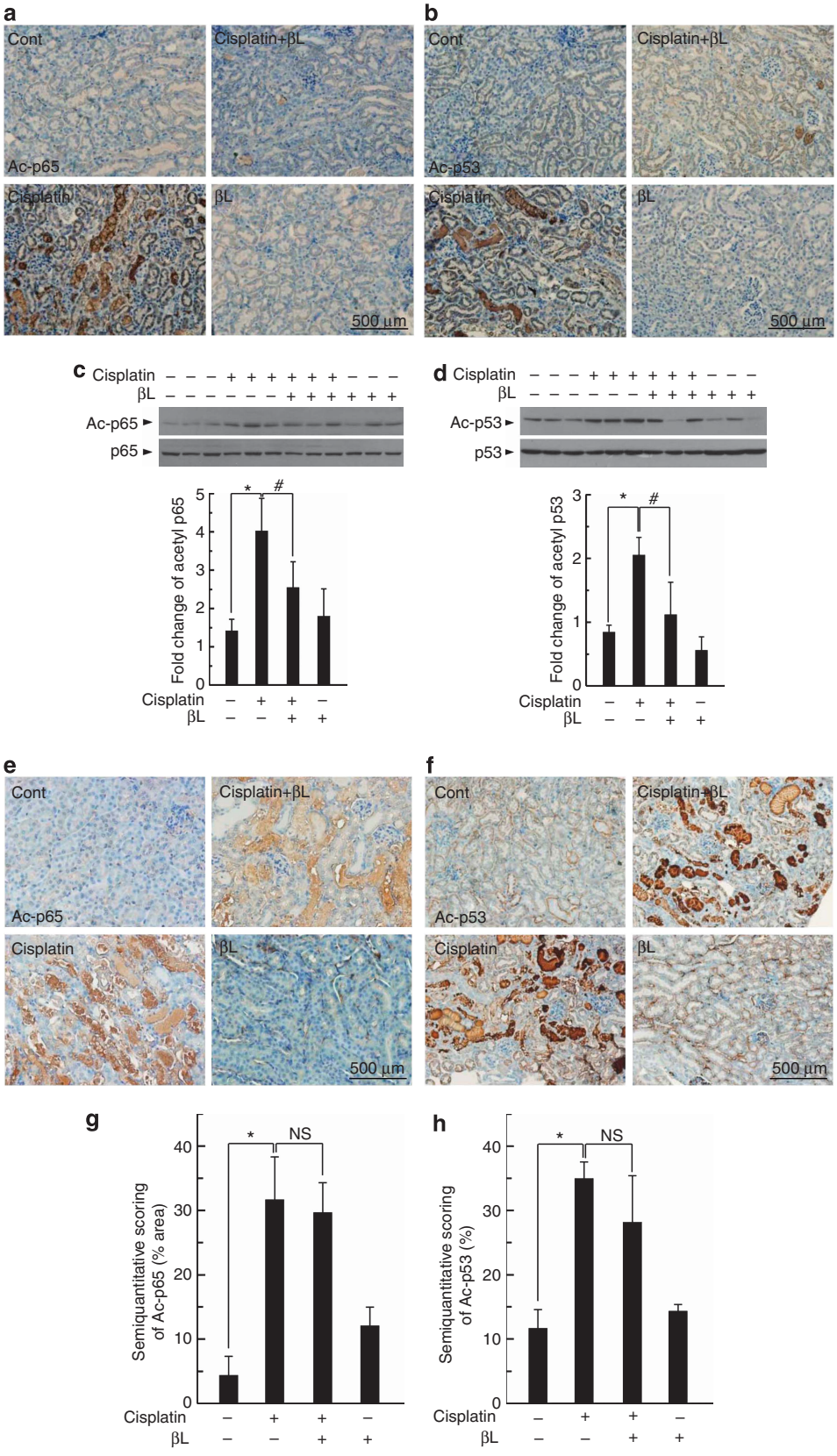
a
Cont
Cisplatin+βL
Ac-p65
Cisplatin
βL
500 μm
b
Cont
Cisplatin+βL
Ac-p53
Cisplatin
βL
500 μm
c
Cisplatin
βL
Ac-p65
p65
Fold change of acetyl p65
d
Cisplatin
βL
Ac-p53
p53
Fold change of acetyl p53
e
Cont
Cisplatin+βL
Ac-p65
Cisplatin
βL
500 μm
f
Cont
Cisplatin+βL
Ac-p53
Cisplatin
βL
500 μm
g
Semiquantitative scoring of Ac-p65 (% area)
NS
h
Semiquantitative scoring of Ac-p53 (%)
NS

of βL. Many studies have revealed that maintaining intracellular NAD^+ is important for cell survival in various diseases, including axonal degeneration, cerebral ischemia, and cardiac hypertrophy. NAD biosynthesis is mainly accomplished through either the *de novo* pathway from tryptophan or the salvage pathway from nicotinamide and nicotinic acid. In addition, NAD^+ can also be converted from NADH by NQO1, which catalyzes two electron reduction of natural substrate such as coenzyme Q-10 or vitamin E, but this reaction rate is very slow. Therefore, it is likely that NQO1 does not take a large part in the regulation of cellular NAD^+ levels in normal state. In fact, we did not find any significant difference in intracellular NAD^+ levels in untreated kidney tissues between WT and $NQO1^{-/-}$ mice (data not shown).

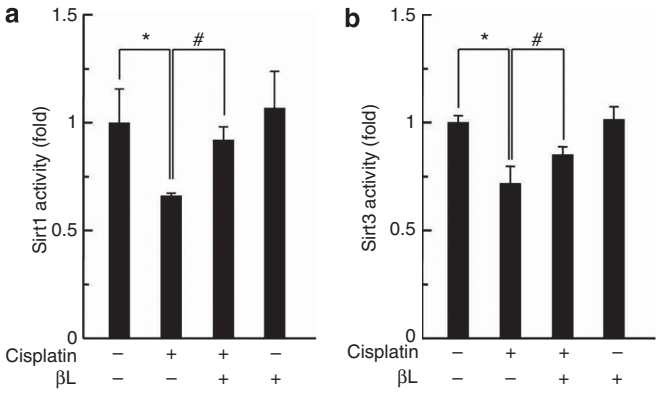

Figure 8 | Effect of βL on Sirt1 and Sirt3 deacetylase activity from kidney tissues of wild-type mice. Kidney tissues were extracted from mice treated as follows: control (Cont), cisplatin, cisplatin + βL, and βL alone. Sirt1 and Sirt3 enzyme activities were analyzed using an assay kit according to the manufacturer's instructions. $^{*,\#}P<0.05$ by one-way analysis of variance compared with the control (*) and cisplatin + βL (#) group ($n=6$).

Recently, numerous studies have reported that the enzymatic activation of NQO1 by βL mediates the beneficial effects on features of metabolic syndromes, including aging, obesity, hypertension, arterial restenosis, and salt-induced renal injury,[30,31,33,34] raising the possibility that intracellular NAD^+ increase through NQO1 activation may be a potential therapeutic target for treating various diseases. In this report, we investigated whether NQO1 enzymatic activation by βL ameliorates cisplatin-induced renal changes. Consistent with previous reports, βL restores the cisplatin-induced reduction of the cellular NAD^+/NADH ratio in renal tissue in WT mice but not in $NQO1^{-/-}$ mice (Figure 6). Interestingly, the major reason for the cellular change in the NAD^+/NADH ratio by βL in WT mice is not the reduction in NADH but the increase in NAD^+ levels (data not shown). Modulation of NAD^+ levels may have a strong impact on metabolic

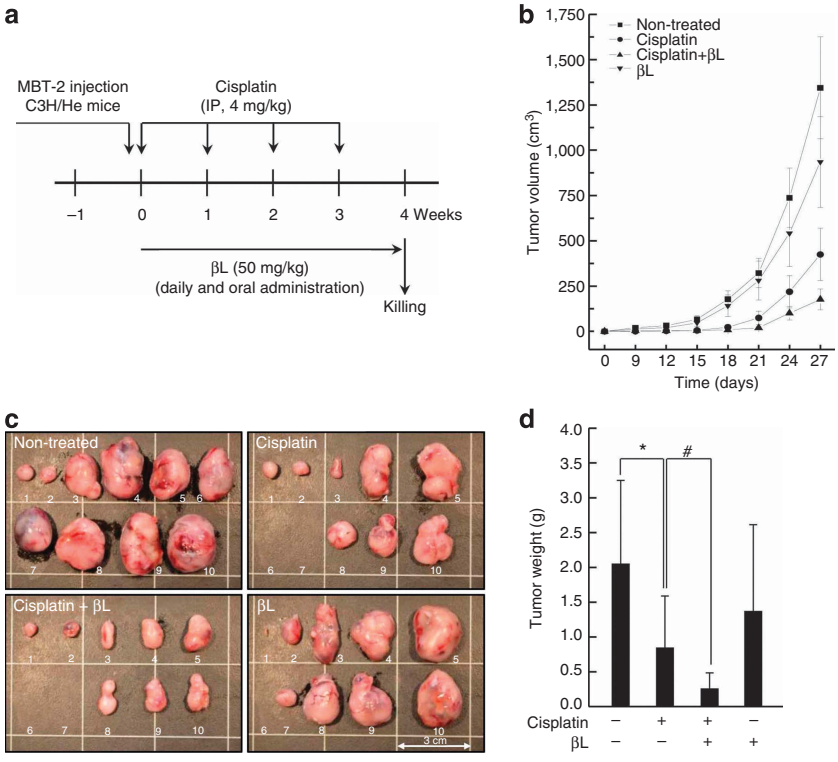

Figure 9 | Effect of βL on cisplatin's tumoricidal activity using a tumor-bearing mouse model. (**a**) Schematic schedule for evaluating the effect of βL on the tumoricidal activity of cisplatin *in vivo*. (**b**–**d**) To evaluate the chemotherapeutic effect of cisplatin with or without βL, tumor volume was measured every 3 days until the time of killing. Tumor mass was removed at 4 weeks after the MBT-2 inoculation, photographed, and weighed. $^{*,\#}P<0.05$ by one-way analysis of variance compared with control (*) and cisplatin + βL (#) group ($n=10$). IP, intraperitoneal.

processes, such as β-oxidation, ATP production, cell signaling, and cellular redox state,[36–39] as NAD^+ acts as a cofactor for various enzymes, including sirtuins and ADP-ribose transferases.[32] Of these, sirtuin proteins use NAD^+ as a substrate to deacetylate various targets, including histones and NF-κB p65 (by Sirt1) in the nucleus,[52] and IDH2 and p53 (by Sirt3) in the mitochondria.[51,57,66] In the case of NF-κB, nuclear translocation itself may cause transcriptional activation of target genes, but additional modification of the p65 subunit by acetylation potentiates its transcriptional activity.[14,15] Furthermore, acetylation and translocation of p53 induces cell death signals, which are normally stabilized by MDM2 (mouse double-minute 2 homolog) in the cytoplasm.[16] We found hyperacetylation of p65 and p53 in cisplatin-treated renal tissues. The hyperacetylation was blocked by βL coadministration in WT mice but sustained in $NQO1^{-/-}$ mice (Figure 7). Surprisingly, Sirt1 and Sirt3 protein expression increased in cisplatin-treated kidney tissues from WT mice, whereas their expression was clearly blocked by βL treatment. However, the increased expression of Sirt1 and Sirt3 induced by cisplatin was not blocked by βL in $NQO1^{-/-}$ mice (Supplementary Figure S5 online). Our results showed that increased intracellular NAD^+ levels through NQO1 activation by βL treatment results in the activation of Sirt1 and Sirt3 and protects against cisplatin-induced acute kidney injury. This effect may be similar to that observed in other reports where Sirt1 activation was achieved by either kidney-specific Sirt1 overexpression[67] or by treatment with resveratrol.[17] However, Kim *et al.*[17] showed that cisplatin alone reduces Sirt1 expression and enzyme activity in contrast to our observation that cisplatin treatment alone strongly increased Sirt1 expression confirmed by western blotting, IHC (Supplementary Figure S5 online), and quantitative reverse transcriptase–PCR (data not shown). Of interest, despite the strong increase in the expression of Sirt1 and Sirt3, enzymatic activities were significantly decreased in the cisplatin group compared with control (Figure 8), consistent with the decreased NAD^+ levels in the cisplatin-treated group (Figure 6). The hyperacetylation of p65 and p53 observed in cisplatin-treated renal tissues from both WT and $NQO1^{-/-}$ mice can be also explained by the decreased deacetylase activity of Sirts in cisplatin-treated tissues, because the amount of NAD^+ is insufficient. Therefore, we speculate that the increased expression of Sirt by cisplatin treatment in our experiment may have resulted as an adaptive response but could not protect against cisplatin-induced acute kidney injury due to both inappropriate induction time/amount of Sirt and decreased NAD^+ levels.

In this study, we demonstrated that βL effectively protects against cisplatin-induced acute kidney injury, suggesting βL as a potential therapeutic agent. However, βL should not interfere with the tumoricidal effect of cisplatin in order to be a potential therapeutic agent against the adverse effects of cisplatin. Therefore, we examined whether βL could affect cisplatin-induced tumoricidal activity using a tumor-bearing mouse model. C3H/He mice were subcutaneously injected with MBT-2 mouse bladder tumor cells and treated with cisplatin and/or βL. As shown in Figure 9, βL did not attenuate the tumoricidal effect of cisplatin, but rather enhanced it.

In conclusion, our study demonstrates that NQO1 enzymatic activation by βL suppresses cisplatin-induced acute kidney injury by downregulating potential damage mediators. Cisplatin causes renal injury through a sequence of events that include tubular cell death and tissue damage by TNF-α secretion and a positive feedback loop of NF-κB activation, oxidative stress, and inflammatory responses. Our data suggest that βL elevates cellular NAD^+ levels through the activation of NQO1. This, in turn, activates the deacetylase enzymes Sirt1 and Sirt3, which deacetylate p65 and p53 in the nuclei and mitochondria, respectively. Taken together, our results strongly suggest pharmacological activation of NQO1 as a potential strategy for preventing cisplatin-induced renal injury.

MATERIALS AND METHODS

Animals and drug treatments

C57BL/6 WT mice were purchased from Orient Bio (Seongnam, Korea). NQO1 knockout mice on a C57BL/6 background were kindly provided by Dr C. H. Lee (Animal Model Center, Korea Research Institute of Bioscience and Biotechnology, Daejeon, Korea). All mice were fed a standard commercial diet while housed at an ambient temperature of 20–22 °C with a relative humidity of 50 ± 5% under 12/12-h light–dark cycle in a specific pathogen-free facility. The experimental mice were 8 weeks old and were divided into four groups: control ($n = 5$), cisplatin (20 mg/kg; Sigma Chemical, St Louis, MO; $n = 5$), βL + cisplatin ($n = 5$), and βL alone (40 mg/kg; $n = 5$). The dose and time of cisplatin treatment for nephrotoxicity were chosen according to a published method.[68,69] βL was administered orally once a day for 4 days. Cisplatin was injected once at 12 h after the first βL administration. The mice were killed at 72 h after the single cisplatin injection. The experimental protocol was approved by the Animal Care and Use Committee at Wonkwang University.

NQO1 enzymatic activity assay

NQO1 activity was measured using kidney cytosolic fractions.[35,70] Briefly, NQO1 activity was calculated by measuring the conversion rate of NADH to NAD^+ using DCPIP (2,6-dichlorophenolindophenol; Sigma) as a substrate. The reduction of NADH was measured at 600 nm over 2 min. NQO1 activity was measured in a 1-ml reaction volume containing kidney cytosolic fractions, 200 μmol/l NADH (Sigma), 40 μmol/l DCPIP, and Tris-HCl buffer (25 mmol/l Tris-HCl, pH 7.4 and 0.7 mg/ml bovine serum albumin). Moreover, dicumarol (Sigma) was used to inhibit NQO1 activation. The sample size for each group was five.

Assays for renal functional markers and proinflammatory cytokines

For renal function analysis, serum was isolated and stored at −80 °C until use. Serum creatinine and BUN levels were measured using an assay kit according to the manufacturer's instructions (BioVision, Milpitas, CA). In addition, the proinflammatory cytokines TNF-α, IL-1β, and IL-6 from serum or homogenates from kidney tissue were quantified by ELISA (Quantikine Kit; R&D Systems,

Minneapolis, MN) according to the manufacturer's instructions. For measuring cytokines, kidney tissue was homogenized in phosphate-buffered saline containing 0.05% Tween-20. Aliquots containing 300 μg of total protein were used. A metabolic cage was used for collecting urine to analyze the level of urinary cytokines. The sample size for each group was five.

Histological analysis and neutrophil counting

Mouse kidneys were fixed in 4% formaldehyde and embedded in paraffin wax. The 5-μm-thick sections were deparaffinized in xylene and rehydrated through graded concentrations of ethanol. H&E and PAS staining were performed using standard protocols. Images were collected and analyzed using a light microscope (IX71, Olympus, Tokyo, Japan) with DP analyzer software (DP70-BSW, Tokyo, Japan). Tubular damage in PAS-stained kidney sections was examined under a light microscope and scored based on the percentage of cortical tubular necrosis: 0 = normal, 1 = 1–10, 2 = 11–25, 3 = 26–45, 4 = 46–75, and 5 = 76–100%. Slides were scored in a blinded manner, and results are means ± s.d. of 10 representative fields/group. Criterion for tubular necrosis displaying the loss of the proximal tubular brush border and cast formation was defined by the methods described previously.[63] The sample size for each group was 10. Neutrophil infiltration was quantitatively assessed on PAS-stained tissue by a renal pathologist by counting the number of neutrophils per high-power field (×400). At least 10 fields were counted in the outer stripe of the outer medulla for each slide.

Immunohistochemical analysis

To determine the expression levels of various target molecules, IHC was performed. In brief, 5-μm-thick kidney sections were deparaffinized and rehydrated through graded concentrations of ethanol. Antigen was retrieved in Tris-EDTA buffer (10 mmol/l Tris base, 1 mmol/l EDTA solution, 0.05% Tween-20, pH 9.0) by using a microwave oven. Endogenous peroxidase activity was quenched by incubation for 5 min in 0.3% H_2O_2 solution. Nonspecific antibody binding was blocked with 1.5% goat or rabbit serum for 30 min, and then sections were incubated with target antibodies to TNF-α, IL-1β, IL-6, Sirt1, Sirt3, p65, NOX1, NOX4 (Santa Cruz Biotechnology, Santa Cruz, CA), Ac-p65 (Abcam, Cambridge, MA), Ac-p53, and p53 (Cell Signaling Technology, Danvers, MA). Sections were washed with phosphate-buffered saline and processed with biotin linkage and a streptavidin kit according to the manufacturer's instructions (LSAB+ System-HRP; Dako, Carpinteria, CA). Target areas were visualized using a DAB+ chromogen substrate solution and counterstained with hematoxylin solution. For semiquantitative analyses on the IHC-processed kidney specimens, images were collected and analyzed using open-source software ImageJ v. 1.46 (Bethesda, MD).

Western blot analysis

To determine the expression levels of target proteins, western blotting was performed. Briefly, kidney tissues were homogenized with lysis buffer (10 mmol/l Tris-HCl pH 7.6, 150 mmol/l NaCl, 1% Triton X-100, 1% sodium deoxycholate,1 mmol/l EDTA, 50 mmol/l β-glycerophosphate, 1 mmol/l dithiothreitol, 1 mmol/l NaF, 1 mmol/l Na_3VO_4, 1 mmol/l phenylmethanesulfonylfluoride, and 1X protease inhibitor cocktail). After centrifugation, the collected lysates were subjected to electrophoresis on 10% SDS-PAGE (sodium dodecyl sulfate-polyacrylamide gel electrophoresis) and then transferred onto a nitrocellulose membrane. The proteins were visualized by a chemiluminescent solution according to the manufacturer's instructions (Supersignal Pico Substrate; Thermo Scientific, Rockford, IL). For measuring NF-κB p65 nuclear translocation, nuclear fraction was prepared using a kit (Sigma-Aldrich, St Louis, MO) according to the manufacturer's instruction and analyzed using p65 antibody (Cell Signaling Technology) and Histone H3 (H3, Cell Signaling Technology) as a loading control. Signaling intensities were quantified by using the ImageJ program. The sample size for each group was three.

Measurement of NAD^+ and NADH concentrations

NAD^+ and NADH (μmol/l/μg protein) were measured in kidney tissues by using a kit (BioAssay Systems, Hayward, CA). Briefly, kidney tissues were homogenized in either acidic extraction buffer (NAD^+ extraction) or alkaline extraction buffer (NADH extraction). Homogenates were heated at 60 °C for 5 min and then neutralized by the addition of the opposite extraction buffer. The optical density was measured at 595 nm after a 15-min incubation at room temperature. Experiments were carried out according to the manufacturer's procedures. The sample size for each group was five.

NADPH oxidase activity

The activity of NADPH oxidase was determined as previously described.[71] Briefly, 50 μg protein of kidney homogenates was incubated with an assay buffer (1 mmol/l ethylene glycol tetraacetic acid and 5 μmol/l lucigenin in phosphate buffer, pH 7.0). The reaction was initiated by the addition of 50 μmol/l NADPH to the incubation mixture. The activity was counted immediately using a tabletop luminometer (Berthold Detection Systems FB Luminometer; Oak Ridge, TN) with sampling time every 6 s. Samples were counted over a period of 5 min, and the fluorescence values were recorded for over 2 min of stable readings and averaged for that sample. The number of sample tissues for each group was six.

Measurement of Sirt1 and Sirt3 activity

The effects of cisplatin and βL on Sirt1 and Sirt3 activity were determined using a fluorescent Sirt1 and Sirt3 assay kit (Enzo Life Sciences International, Plymouth Meeting, PA). Briefly, the Sirt1 activity assays were performed with kidney homogenates (20 μg of protein) and Fluor de Lys-Sirt1 as the substrate in Sirt1 assay buffer (25 mmol/l Tris-Cl, pH 8.0, 137 mmol/l NaCl, 2.7 mmol/l KCl, 1 mmol/l $MgCl_2$, and 1 mg/ml bovine serum albumin), and the Sirt3 activity assays were performed using Fluor de Lys-Sirt3 as the substrate in Sirt3 assay buffer (50 mmol/l Tris-Cl, pH 8.0, 137 mmol/l NaCl, 2.7 mmol/l KCl, 1 mmol/l $MgCl_2$, and 1 mg/ml bovine serum albumin) in a 96-well plate. Reactions were initiated by adding each substrate solution. After incubation at 37 °C for 1 h, the plate was further incubated with developing solution for 5 min. Fluorescence readings were obtained using the CytoFluor series 4000 fluorometer (Perseptive Biosystems, Framingham, MA) with the excitation wavelength set to 360 nm and the emission to 460 nm. The sample size for each group was six.

Statistical analysis

Experiment sample sizes are individually indicated in the Method sections and the corresponding figure legends. All values are represented as mean ± s.d. One-way analysis of variance was used to calculate the statistical significance of the results, and *P*-values <0.05 are considered statistically significant.

DISCLOSURE

All the authors declared no competing interests.

ACKNOWLEDGMENTS

This work was supported by the two National Research Foundation of Korea (NRF) grants funded by the Korean government (MEST): (No. 2011-0028866) and (No. 2011-0030715).

SUPPLEMENTARY MATERIAL

Figure S1. Enzymatic activation of NQO1 and modulation of intracellular NAD^+/NADH ratio by βL in kidney tissues.
Figure S2. Schematic schedule for the *in vivo* experiment.
Figure S3. Effect of βL on the cisplatin-induced expression of proinflammatory cytokines IL-1β and IL-6 in renal tissue from WT mice.
Figure S4. Effect of βL on the cisplatin-induced expression of proinflammatory cytokines IL-1β and IL-6 in renal tissue from $NQO1^{-/-}$ mice.
Figure S5. Effect of βL on Sirt1 and Sirt3 expression levels in renal tissues from WT and $NQO1^{-/-}$ mice.
Supplementary material is linked to the online version of the paper at http://www.nature.com/ki

REFERENCES

1. Rosenberg B, Vancamp L, Krigas T. Inhibition of cell division in *Escherichia coli* by electrolysis products from a platinum electrode. *Nature* 1965; **205**: 698–699.
2. Wang D, Lippard SJ. Cellular processing of platinum anticancer drugs. *Nat Rev Drug Discov* 2005; **4**: 307–320.
3. Cohen SM, Lippard SJ. Cisplatin: from DNA damage to cancer chemotherapy. *Prog Nucleic Acid Res Mol Biol* 2001; **67**: 93–130.
4. Arany I, Safirstein RL. Cisplatin nephrotoxicity. *Semin Nephrol* 2003; **23**: 460–464.
5. Siddik ZH. Cisplatin: mode of cytotoxic action and molecular basis of resistance. *Oncogene* 2003; **22**: 7265–7279.
6. Pabla N, Dong Z. Cisplatin nephrotoxicity: mechanisms and renoprotective strategies. *Kidney Int* 2008; **73**: 994–1007.
7. Kuriakose GC, Kurup MG. Evaluation of renoprotective effect of Aphanizomenon flos-aquae on cisplatin-induced renal dysfunction in rats. *Ren Fail* 2008; **30**: 717–725.
8. Luke DR, Vadiei K, Lopez-Berestein G. Role of vascular congestion in cisplatin-induced acute renal failure in the rat. *Nephrol Dial Transplant* 1992; **7**: 1–7.
9. Ciccarelli RB, Solomon MJ, Varshavsky A *et al.* In vivo effects of cis- and trans-diamminedichloroplatinum(II) on SV40 chromosomes: differential repair, DNA-protein cross-linking, and inhibition of replication. *Biochemistry* 1985; **24**: 7533–7540.
10. Heiger-Bernays WJ, Essigmann JM, Lippard SJ. Effect of the antitumor drug cis-diamminedichloroplatinum (II) and related platinum complexes on eukaryotic DNA replication. *Biochemistry* 1990; **29**: 8461–8466.
11. Zamble DB, Lippard SJ. Cisplatin and DNA repair in cancer chemotherapy. *Trends Biochem Sci* 1995; **20**: 435–439.
12. Jamieson ER, Lippard SJ. Structure, recognition, and processing of cisplatin-DNA adducts. *Chem Rev* 1999; **99**: 2467–2498.
13. Eastman A. The formation, isolation and characterization of DNA adducts produced by anticancer platinum complexes. *Pharmacol Ther* 1987; **34**: 155–166.
14. Huang B, Yang XD, Lamb A *et al.* Posttranslational modifications of NF-kappaB: another layer of regulation for NF-kappaB signaling pathway. *Cell Signal* 2010; **22**: 1282–1290.
15. Ghizzoni M, Haisma HJ, Maarsingh H *et al.* Histone acetyltransferases are crucial regulators in NF-kappaB mediated inflammation. *Drug Discov Today* 2011; **16**: 504–511.
16. Taira N, Yoshida K. Post-translational modifications of p53 tumor suppressor: determinants of its functional targets. *Histol Histopathol* 2012; **27**: 437–443.
17. Kim DH, Jung YJ, Lee JE *et al.* SIRT1 activation by resveratrol ameliorates cisplatin-induced renal injury through deacetylation of p53. *Am J Physiol Renal Physiol* 2011; **301**: F427–F435.
18. Ross D, Kepa JK, Winski SL *et al.* NAD(P)H:quinone oxidoreductase 1 (NQO1): chemoprotection, bioactivation, gene regulation and genetic polymorphisms. *Chem Biol Interact* 2000; **129**: 77–97.
19. Gaikwad A, Long DJ 2nd, Stringer JL *et al.* In vivo role of NAD(P)H:quinone oxidoreductase 1 (NQO1) in the regulation of intracellular redox state and accumulation of abdominal adipose tissue. *J Biol Chem* 2001; **276**: 22559–22564.
20. Kim KH, Lyu JH, Koo ST *et al.* MyD88 is a mediator for the activation of Nrf2. *Biochem Biophys Res Commun* 2011; **404**: 46–51.
21. Gao M, Singh A, Macri K *et al.* Antioxidant components of naturally-occurring oils exhibit marked anti-inflammatory activity in epithelial cells of the human upper respiratory system. *Respir Res* 2011; **12**: 92.
22. Gessner DK, Ringseis R, Siebers M *et al.* Inhibition of the pro-inflammatory NF-kappaB pathway by a grape seed and grape marc meal extract in intestinal epithelial cells. *J Anim Physiol Anim Nutr (Berl)* 2012; **96**: 1074–1083.
23. Pazdro R, Burgess JR. The antioxidant 3H-1,2-dithiole-3-thione potentiates advanced glycation end-product-induced oxidative stress in SH-SY5Y cells. *Exp Diabetes Res* 2012; **2012**: 137607.
24. Jones CI 3rd, Zhu H, Martin SF *et al.* Regulation of antioxidants and phase 2 enzymes by shear-induced reactive oxygen species in endothelial cells. *Ann Biomed Eng* 2007; **35**: 683–693.
25. Moscovitz O, Tsvetkov P, Hazan N *et al.* A mutually inhibitory feedback loop between the 20S proteasome and its regulator, NQO1. *Mol Cell* 2012; **47**: 76–86.
26. Chiu MM, Ko YJ, Tsou AP *et al.* Analysis of NQO1 polymorphisms and p53 protein expression in patients with hepatocellular carcinoma. *Histol Histopathol* 2009; **24**: 1223–1232.
27. Nioi P, Hayes JD. Contribution of NAD(P)H:quinone oxidoreductase 1 to protection against carcinogenesis, and regulation of its gene by the Nrf2 basic-region leucine zipper and the arylhydrocarbon receptor basic helix-loop-helix transcription factors. *Mutat Res* 2004; **555**: 149–171.
28. Pardee AB, Li YZ, Li CJ. Cancer therapy with beta-lapachone. *Curr Cancer Drug Targets* 2002; **2**: 227–242.
29. Planchon SM, Wuerzberger S, Frydman B *et al.* Beta-lapachone-mediated apoptosis in human promyelocytic leukemia (HL-60) and human prostate cancer cells: a p53-independent response. *Cancer Res* 1995; **55**: 3706–3711.
30. Hwang JH, Kim DW, Jo EJ *et al.* Pharmacological stimulation of NADH oxidation ameliorates obesity and related phenotypes in mice. *Diabetes* 2009; **58**: 965–974.
31. Kim SY, Jeoung NH, Oh CJ *et al.* Activation of NAD(P)H:quinone oxidoreductase 1 prevents arterial restenosis by suppressing vascular smooth muscle cell proliferation. *Circ Res* 2009; **104**: 842–850.
32. Houtkooper RH, Canto C, Wanders RJ *et al.* The secret life of NAD+: an old metabolite controlling new metabolic signaling pathways. *Endocr Rev* 2010; **31**: 194–223.
33. Kim YH, Hwang JH, Noh JR *et al.* Activation of NAD(P)H:quinone oxidoreductase ameliorates spontaneous hypertension in an animal model via modulation of eNOS activity. *Cardiovasc Res* 2011; **91**: 519–527.
34. Lee JS, Park AH, Lee SH *et al.* Beta-lapachone, a modulator of NAD metabolism, prevents health declines in aged mice. *PLoS One* 2012; **7**: e47122.
35. Kim YH, Hwang JH, Noh JR *et al.* Prevention of salt-induced renal injury by activation of NAD(P)H:quinone oxidoreductase 1, associated with NADPH oxidase. *Free Radic Biol Med* 2012; **52**: 880–888.
36. Oka S, Hsu CP, Sadoshima J. Regulation of cell survival and death by pyridine nucleotides. *Circ Res* 2012; **111**: 611–627.
37. Ussher JR, Jaswal JS, Lopaschuk GD. Pyridine nucleotide regulation of cardiac intermediary metabolism. *Circ Res* 2012; **111**: 628–641.
38. Abdellatif M. Sirtuins and pyridine nucleotides. *Circ Res.* 2012; **111**: 642–656.
39. Kitada M, Kume S, Takeda-Watanabe A *et al.* Sirtuins and renal diseases: relationship with aging and diabetic nephropathy. *Clin Sci (Lond)* 2013; **124**: 153–164.
40. Hassa PO, Haenni SS, Elser M *et al.* Nuclear ADP-ribosylation reactions in mammalian cells: where are we today and where are we going? *Microbiol Mol Biol Rev* 2006; **70**: 789–829.
41. Hara N, Yamada K, Shibata T *et al.* Elevation of cellular NAD levels by nicotinic acid and involvement of nicotinic acid phosphoribosyltransferase in human cells. *J Biol Chem* 2007; **282**: 24574–24582.
42. Imai S, Kiess W. Therapeutic potential of SIRT1 and NAMPT-mediated NAD biosynthesis in type 2 diabetes. *Front Biosci* 2009; **14**: 2983–2995.
43. Belenky P, Bogan KL, Brenner C. NAD+ metabolism in health and disease. *Trends Biochem Sci* 2007; **32**: 12–19.
44. Howitz KT, Bitterman KJ, Cohen HY *et al.* Small molecule activators of sirtuins extend *Saccharomyces cerevisiae* lifespan. *Nature* 2003; **425**: 191–196.

45. Lin SJ, Kaeberlein M, Andalis AA *et al.* Calorie restriction extends *Saccharomyces cerevisiae* lifespan by increasing respiration. *Nature* 2002; **418**: 344–348.
46. Fulco M, Cen Y, Zhao P *et al.* Glucose restriction inhibits skeletal myoblast differentiation by activating SIRT1 through AMPK-mediated regulation of Nampt. *Dev Cell* 2008; **14**: 661–673.
47. Kim D, Nguyen MD, Dobbin MM *et al.* SIRT1 deacetylase protects against neurodegeneration in models for Alzheimer's disease and amyotrophic lateral sclerosis. *EMBO J* 2007; **26**: 3169–3179.
48. Michan S, Sinclair D. Sirtuins in mammals: insights into their biological function. *Biochem J* 2007; **404**: 1–13.
49. Luo J, Nikolaev AY, Imai S *et al.* Negative control of p53 by Sir2alpha promotes cell survival under stress. *Cell* 2001; **107**: 137–148.
50. Motta MC, Divecha N, Lemieux M *et al.* Mammalian SIRT1 represses forkhead transcription factors. *Cell* 2004; **116**: 551–563.
51. Vaziri H, Dessain SK, Ng Eaton E *et al.* hSIR2(SIRT1) functions as an NAD-dependent p53 deacetylase. *Cell* 2001; **107**: 149–159.
52. Yeung F, Hoberg JE, Ramsey CS *et al.* Modulation of NF-kappaB-dependent transcription and cell survival by the SIRT1 deacetylase. *EMBO J* 2004; **23**: 2369–2380.
53. Yoshizaki T, Milne JC, Imamura T *et al.* SIRT1 exerts anti-inflammatory effects and improves insulin sensitivity in adipocytes. *Mol Cell Biol* 2009; **29**: 1363–1374.
54. Shi T, Wang F, Stieren E *et al.* SIRT3, a mitochondrial sirtuin deacetylase, regulates mitochondrial function and thermogenesis in brown adipocytes. *J Biol Chem* 2005; **280**: 13560–13567.
55. Ahn BH, Kim HS, Song S *et al.* A role for the mitochondrial deacetylase Sirt3 in regulating energy homeostasis. *Proc Natl Acad Sci USA* 2008; **105**: 14447–14452.
56. Yang H, Yang T, Baur JA *et al.* Nutrient-sensitive mitochondrial NAD + levels dictate cell survival. *Cell* 2007; **130**: 1095–1107.
57. Li S, Banck M, Mujtaba S *et al.* p53-induced growth arrest is regulated by the mitochondrial SirT3 deacetylase. *PLoS One* 2010; **5**: e10486.
58. Kuhlmann MK, Burkhardt G, Kohler H. Insights into potential cellular mechanisms of cisplatin nephrotoxicity and their clinical application. *Nephrol Dial Transplant* 1997; **12**: 2478–2480.
59. Kroning R, Lichtenstein AK, Nagami GT. Sulfur-containing amino acids decrease cisplatin cytotoxicity and uptake in renal tubule epithelial cell lines. *Cancer Chemother Pharmacol* 2000; **45**: 43–49.
60. Taguchi T, Nazneen A, Abid MR *et al.* Cisplatin-associated nephrotoxicity and pathological events. *Contrib Nephrol* 2005; **148**: 107–121.
61. Ramesh G, Reeves WB. TNF-alpha mediates chemokine and cytokine expression and renal injury in cisplatin nephrotoxicity. *J Clin Invest* 2002; **110**: 835–842.
62. Sung MJ, Kim DH, Jung YJ *et al.* Genistein protects the kidney from cisplatin-induced injury. *Kidney Int* 2008; **74**: 1538–1547.
63. Faubel S, Lewis EC, Reznikov L *et al.* Cisplatin-induced acute renal failure is associated with an increase in the cytokines interleukin (IL)-1beta, IL-18, IL-6, and neutrophil infiltration in the kidney. *J Pharmacol Exp Ther* 2007; **322**: 8–15.
64. Zhu H, Li Y. NAD(P)H: quinone oxidoreductase 1 and its potential protective role in cardiovascular diseases and related conditions. *Cardiovasc Toxicol* 2012; **12**: 39–45.
65. Radjendirane V, Joseph P, Lee YH *et al.* Disruption of the DT diaphorase (NQO1) gene in mice leads to increased menadione toxicity. *J Biol Chem* 1998; **273**: 7382–7389.
66. Yu W, Dittenhafer-Reed KE, Denu JM. SIRT3 protein deacetylates isocitrate dehydrogenase 2 (IDH2) and regulates mitochondrial redox status. *J Biol Chem* 2012; **287**: 14078–14086.
67. Hasegawa K, Wakino S, Yoshioka K *et al.* Kidney-specific overexpression of Sirt1 protects against acute kidney injury by retaining peroxisome function. *J Biol Chem* 2010; **285**: 13045–13056.
68. Lee S, Kim W, Moon SO *et al.* Rosiglitazone ameliorates cisplatin-induced renal injury in mice. *Nephrol Dial Transplant* 2006; **21**: 2096–2105.
69. Lee S, Moon SO, Kim W *et al.* Protective role of L-2-oxothiazolidine-4-carboxylic acid in cisplatin-induced renal injury. *Nephrol Dial Transplant* 2006; **21**: 2085–2095.
70. Lickteig AJ, Fisher CD, Augustine LM *et al.* Genes of the antioxidant response undergo upregulation in a rodent model of nonalcoholic steatohepatitis. *J Biochem Mol Toxicol* 2007; **21**: 216–220.
71. Kim HJ, Lee JH, Kim SJ *et al.* Roles of NADPH oxidases in cisplatin-induced reactive oxygen species generation and ototoxicity. *J Neurosci* 2010; **30**: 3933–3946.